A MARKOV RANDOM FIELD MODEL FOR BILEVEL CUTSET RECONSTRUCTION

Shengxin Zha, Thrasyvoulos N. Pappas

EECS Department, Northwestern University, Evanston, IL 60208

ABSTRACT

Index Terms—

1. INTRODUCTION

MRF ...

Bilevel image reconstruction ...

Previous work ...

Proposed model ...

The main contributions include (i) a 3-point-clique MRF model that tolerant slow changes; (ii) a hybrid MRF model that ensures the independency between cutset blocks and keeps the sensitivity to change near block boundaries; and (iii) a two-stage cutset reconstruction algorithm.

Paper structure ...

2. PREVIOUS WORK

2.1. MRF with 2-pt cliques

A bilevel image can be modeled by the Markov random field (MRF). Let $G = (V, E)$ be an 8-connected graph, where V and E denote the nodes (vertices) and edges, modeling the pixels and the connectivities in an image, respectively. The MRF with 2-point cliques is defined on the 8-connected graph. The 2-point cliques consist of horizontal, vertical and diagonal neighboring nodes (Figure 1a). A node is associated with 8 cliques (Figure 1b).

Let x_s denote the value at pixel s. Given the MRF model, the image values **x** are realized by maximizing the probability

$$p(\mathbf{x}) = \frac{1}{Z} \exp\{-\sum_C V_C(\mathbf{x})\}, \quad \mathbf{x} \in \{0, 1\} \quad (1)$$

$$V_C(\mathbf{x}) = \begin{cases} -\beta, & x_s = x_q, (s,q) \in C, \beta > 0 \\ +\beta, & x_s \neq x_q, (s,q) \in C, \beta > 0 \end{cases} \quad (2)$$

where Z is a normalization constant, C denotes the collection of cliques, and q denotes a neighboring node of s. Such model has been used in cutset reconstruction of bilevel images [1, 2].

2.2. Cutset-MRF

The term *cutset* was first proposed in lossy bilevel image compression that relies on the reconstruction of bilevel images

(a) 2-pt cliques

(b) A node (blue) associated with 8 cliques
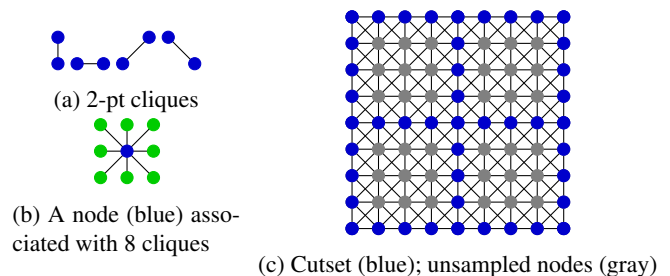
(c) Cutset (blue); unsampled nodes (gray)

Fig. 1: MRF and cutset associated with 2-point cliques

from cutsets. Given a 2D Cartesian grid, a A cutset typically takes samples on evenly spaced rows and columns of a 2D Cartesian grid (e.g. Figure 1c, sampling step $N = 4$). The grid can be decoupled into $(N + 1) \times (N + 1)$ blocks, consisting of $4N$ cutset nodes on the shared block boundaries and $(N-1) \times (N-1)$ unsampled nodes in the block interior. Based on the 2-point-clique MRF model, the interior nodes can be completely described by the cutset nodes that enclose them. Therefore, the inferring of unsampled nodes in each block is independent with other blocks. The optimization under MRF model is thus reduced to seeking optimal path(s) that partition the block interior given the boundary.

In complicated blocks, however, the optimal partition in MRF sense may not lead to a truthful reconstruction. Thus, additional *connection bits* are encoded to improve the choice of partition paths in bilevel image compression where the original images are accessible [1, 2]. Figure 3 shows examples when the connection bits are needed. The connection bits indicate which runs of same valued nodes on block to connect via the interior nodes. For example, two black runs are connected in the first reconstruction example in Figure 3d while two white runs are connected in the second reconstruction example.

3. PROPOSED APPROACH

3.1. Cutset-MRF Graph Partition

The reconstruction of the block interiors given the block boundaries can be reinterpreted as graph partition that optimizes the following: (i) the connection of runs that used as graph partition roots; and (ii) the optimal graph partition paths given the connection of runs. After partition, the edges between neighboring nodes of different values are being removed, result in disconnected subgraphs (representing the reconstructed segments). A *graph partition* path is referred to as a polyline that cut the edges during the graph partition process.

The cutset-MRF with connection bit approach satisfies these two stages of graph partition: the connection bits indicate which runs to connect; while the 2-point-clique MRF model generates the optimal graph partition paths given the connection bits. The connection bits, however, can not be obtained in actual image reconstruction applications where the originals are not available. Without the connection bits, the 2-point-clique MRF model alone is bias towards shorter partition paths, thus fails to provide a realistic graph partition model.

To address these issues, we propose a novel two stage cutset-MRF approach that optimizes the graph partition without any reference image. More specifically, it consists of a 2-point-clique MRF model that optimizes the graph partition paths given each possible connection of runs and a hybrid MRF model optimizes the connection. The hybrid MRF model includes a 3-point-clique MRF model that aims to eliminate the bias towards shorter graph partition paths and consequently allows the segments on the block boundary to extend into the block interior and a complimentary 2-point-clique MRF model active only near the block boundary.

3.2. 3-point-clique MRF Model

The main draw back the 2-point-clique MRF model is that it penalizes any change of values in a clique of neighboring nodes, thus discourages the formation of segments. We propose a 3-point-clique MRF model that allows the values to change slowly across the field.

Assume the graph is infinite. We define a MRF model associated with a 3-point-clique function

$$V_C(\mathbf{x}) = \begin{cases} \beta_0, & x_{s_{-1}} = x_{s_0} = x_{s_{+1}} \\ \beta_1, & x_{s_{-1}} \neq x_{s_0} \neq x_{s_{+1}} \\ \beta_2, & o.w. \end{cases} \quad (3)$$

where C denotes a collection of 3-point cliques, including the horizontally, vertically and diagonally connected 3 nodes (Figure 2a); $s_{-1,0,+1} \in C$; s_0 is the clique center node; and $\beta_{0,1,2} \in \Re$. A node s in an infinite graph is associated with 12 (3 horizontal, 3 vertical and 6 diagonal) 3-point cliques
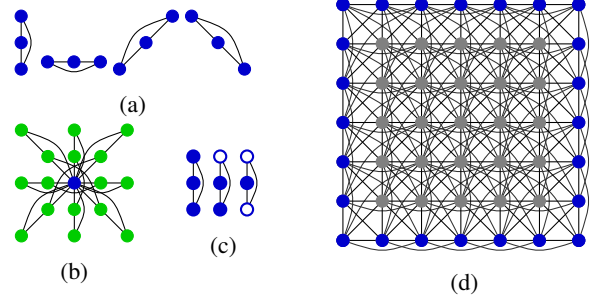

Fig. 2: MRF with 3-point cliques. (a) 3-point cliques, including the horizontally, vertically and diagonally connected 3 nodes. (b) the neighborhood associated with the 3-point cliques with current node denoted in blue and neighboring nodes denoted in green. (c) the three conditions in equation (4): no change, slow change and fast change; the colors are interchangeable. (d) MRF model defined with 3-point cliques in the graph and 2-point cliques at the boundary.

(Figure 2b). The conditions for β_0, β_2 and β_1 model the uniform, slow change and fast change of values within a clique (Figure 2c). It is intuitive to encourage uniform clique by setting $\beta_0 < 0$ and $discourage fast change by setting \beta_1 > 0$. We propose a special case of equation (3) that treats the slow change and uniform cliques equally while penalizes the fast change:

$$V_C(\mathbf{x}) = \begin{cases} +\beta, & x_{s_{-1}} \neq x_{s_0} \neq x_{s_{+1}} \\ -\beta, & o.w. \end{cases} \quad (4)$$

where $s_{-1,0,+1}$ and C are the same as in equation (3) and $\beta > 0$. It is a special case of (3) by setting $\beta_0 = \beta_2 = -\beta$ and $\beta_1 = +\beta$.

The main difference from previous work is that rather than penalizing any change, only fast change is penalized. Consequently, there's no bias towards shorter graph partition paths.

3.3. Boundary Condition

Based on the 3-point-clique MRF model, a cutset can be decoupled into blocks to reconstruct the interior independently from other blocks only if the cutset and the shared block boundaries are two-node-wide. Otherwise, the reconstruction of the entire image has to be optimized simultaneously, not guaranteed with a closed form solution. We propose a hybrid MRF model by replacing the 3-point cliques with 2-point cliques where the boundary violates the interdependency under the 3-point-clique MRF model. The modified clique function is

$$V_C(\mathbf{x}) = \begin{cases} \eta_3 V_{C_3}, & \text{3-pt-clique available} \\ \eta_2 V_{C_2}, & o.w. \end{cases} \quad (5)$$

where V_{C_2} and V_{C_3} are specified in equation (2) and (4), respectively; and $\eta_2, \eta_3 > 0$ are scaling factors. The resulted

graphical model of a one-node-wide cutset block is shown in Figure 2d. The proposed hybrid model ensures the independency between cutset blocks.

Moreover, it is intuitive to extend the boundary value into the neighboring interior nodes while allow some freedom of value change away from the boundary where the nodes are not directly connected to the boundary nodes. The proposed hybrid model is sensitive to any change near block boundary while tolerant to slow change elsewhere.

3.4. Algorithm

The maximization of $p(\mathbf{x})$ in equation (1) is equivalent to the minimization of MRF energy $E = \sum_C V_C(\mathbf{x})$ for all $\mathbf{x}$. Therefore we express the optimization problem in terms of MRF energy minimization. The reconstruction of a cutset block is summarized in Algorithm 1. If multiple $\mathbf{x}_i$ exist for

---

Algorithm 1 Cutset-MRF Graph Partition

Require: Block boundary specification $\mathbf{b}$, MRF parameter β, η_2, η_3
Ensure: The optimal realization of nodes $\mathbf{x}$ in the block
1: **procedure** RECONSTRUCT($\mathbf{b}, \mathbf{x}$)
2:     **for** i-th combination of connection of runs **do**
3:         Find $\mathbf{x}_i$ s.t. $\arg \min E$ with V_C in (2)
4:     **end for**
5:     Find $\mathbf{x} \in \{\mathbf{x}_i\}$ s.t. $\arg \min E$ with V_C in (5)
6:     **return** $\mathbf{x}$
7: **end procedure**

---

a given i, we choose the straight line partition because it is one of the optimal solution in 2-point-clique MRF sense and is supported by statistical result in [3]. If multiple $\mathbf{x}$ exist, we use one of the optimal solutions.

4. EXPERIMENTAL RESULTS

4.1. MRF Model Analysis

We analyze the MRF models in the second stage of graph partition algorithm. Figure 3 demonstrate several typical examples of different optimal reconstructions to the same block boundary specification based on different MRF models. The proposed 3-point-clique MRF model with 2-point-clique boundary condition differs from the 2-point-clique MRF model in reconstruction a, c and e. In these examples, the 2-point-clique MRF model prefers short partition paths (connecting black runs); while the proposed model tolerant the slow change to form segments in block interior but focus on the change between boundary nodes and interior nodes, thus reduces the disconnected flat runs in reconstruction. It leads to substantial improvement in continuity of segments, shown in Figure 4. As for the design the clique function, both V_{C_3} and V_{C_2} in equation (5) are important. The former ensures the fair comparison of partition paths regardless of their length (e.g. Figure 3a) while avoid fast change of node values (e.g. Figure 3bc). The latter is sensitive to the change between boundary nodes and interior nodes, which is essential to extending the value of boundary nodes to interior. It is also important to treat slow change and uniform cliques equally in non-boundary condition. The alternative designs of the 3-point clique function V_{C_3}, such as $(\beta_0, \beta_1, \beta_2) = (-\beta, 0, +\beta)$ or $(\beta_0, \beta_1, \beta_2) = (-\beta, +\beta, +\beta)$ in equation (3), behave essentially like the 2-point clique function in equation (2), thus are bias towards shorter partition paths.

4.2. Visual Result

Figure 4 illustrate examples of cutset reconstruction based on the 2-point-clique MRF model and the proposed hybrid MRF model. The reconstructions from 2-point-clique MRF are obtained with our extension of [1] that considers up to four black and white runs as compared to two in the original work. The MRF parameters are $\beta = 1, \eta_2 = \eta_3 = 1$. The proposed MRF model is insensitive to parameters as long as they satisfy $\beta > 0, \eta_2 > 0, \eta_3 > 0$. The cutsets are obtained at sampling step $N = 8$ (a typical sampling step) and 16 (a challenging sampling step). It demonstrate that the proposed approach substantially improves the reconstruction. The proposed approach makes better decision in whether to connect flat runs (e.g. the fourth row in Figure 4). The improvement of the example the second row mainly comes from the types of block with a nearly flat corner run, corresponding to block reconstruction example in Figure 3e. There are some cases that the connection of runs can not be determined accurately without any extra information (e.g. the broken branches in the example of Figure 4).
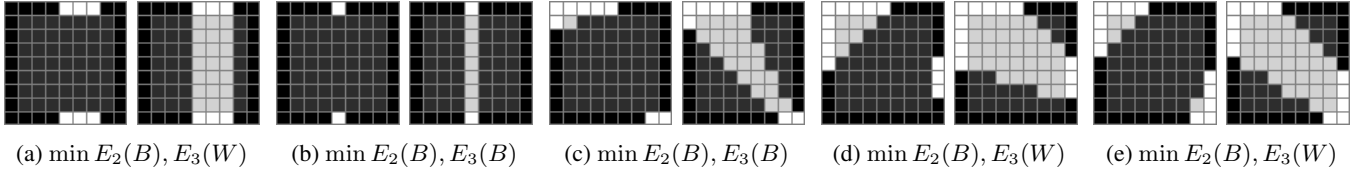
(a) min $E_2(B), E_3(W)$ (b) min $E_2(B), E_3(B)$ (c) min $E_2(B), E_3(B)$ (d) min $E_2(B), E_3(W)$ (e) min $E_2(B), E_3(W)$

Fig. 3: Compare MRF models in reconstruction. B and W denote the reconstruction resulted from connecting black and white runs, resp. min $E_{2,3}$ refers to the minimal (optimal) MRF energy based on the model in [1] and the proposed model.

Table 1: Comparison with other approaches in reconstruction error rate

Dataset	N	unsupervised					supervised
		[4]	[5]	[1]	[1] ext.	proposed	[3]
our bilevel image dataset	16	.075	.069	.075	.075	.049	.047
	14	.065	.061	.063	.063	.042	.039
	12	.056	.053	.051	.052	.034	.031
	10	.047	.044	.039	.038	.027	.024
	8	.038	.035	.030	.027	.019	.017
	6	.027	.025	.016	.015	.013	.011
	4	.015	.015	.007	.007	.007	.007
	2	.005	.003	.002	.002	.002	.002
bilevel shape dataset [6]	16	.064	.054	.049	.047	.043	.039
	14	.056	.047	.041	.040	.036	.033
	12	.048	.042	.033	.033	.029	.026
	10	.040	.035	.025	.025	.023	.020
	8	.032	.029	.019	.018	.017	.015
	6	.022	.020	.013	.013	.012	.011
	4	.012	.012	.006	.006	.006	.006
	2	.003	.002	.002	.002	.002	.002

4.3. Comparison of Approaches in Reconstruction Error

We tested the propose approach on an in-house bilevel image dataset containing 13 complicated bilevel images and a large bilevel shape dataset [6] containing 5578 images. The proposed approach is compared with the 2-point-clique MRF approach [1] and its extension, two baseline inpainting approaches [4, 5] that adapted to bilevel images and a supervised pattern-based approach [3] at various cutset sampling steps ($N = \{16, 14, 12, 10, 8, 6, 4, 2\}$), shown demonstrated in Table 1. The cutset sampling is efficient when the number of sampled nodes is less than the unsampled ones, i.e. when $N >= 6$. It demonstrates that the proposed hybrid MRF approach substantially outperforms other unsupervised methods when $N >= 6$. For completeness of the paper, the proposed approach is also compared with a supervised approach that utilizes the statistics from a dataset of segmented images. The proposed approach largely reduces the gap towards the supervised approach even though the reconstruction in the proposed approach is only based on the boundary specifications.

4.4. Computational Cost

The proposed approach is quite efficient in terms of computational cost. The straight line partition is within optimal solutions in terms of 2-point-clique MRF, thus Algorithm 1 line 3 has a closed form solution and can be reduced to implementation of Bresenham's line. The combinations of connection of runs are limited, therefore, Algorithm 1 line 5 only computes equation (5) for a limited number of times, which mainly consist of summation and comparison. Compared with the approach in [1], the additional computations are introduced by the 3-point clique function, which is quite light weighted. In contrast the inpainting approaches [4, 5] and the pattern-based approach [3] requires much more computational resources.

5. CONCLUSION

In this paper, we proposed a 3-point-clique MRF model and two stage algorithm for reconstructing bilevel images from cutsets. Moreover, we adapt the 3-point-clique MRF model to a hybrid MRF model for one-node-wide cutsets. The proposed approach leads to substantial improvement over previous cutset-MRF approaches in both visual quality and reconstruction error rate. It yields the new state-of-the-art in unsupervised bilevel cutset reconstruction and largely reduces the gap towards the supervised method. The cutset-MRF approaches are computationally efficient. We believe the cutset reconstruction can be further improved by introducing global information or statistical information.

6. REFERENCES

[1] Matthew G. Reyes, Xiaonan Zhao, David L. Neuhoff, and Thrasyvoulos N. Pappas, "Lossy compression of bilevel images based on Markov random fields," in *Proc. Int. Conf. Image Processing (ICIP-07)*, San Antonio, TX, Sept. 2007, vol. 2, pp. II–373–II–376.

[2] Shengxin Zha, Thrasyvoulos N. Pappas, and David L. Neuhoff, "Hierarchical bilevel image compression based on cutset sampling," in *Proc. Int. Conf. Image Processing (ICIP)*, Orlando, FL, Oct. 2012, pp. 2517–2520.

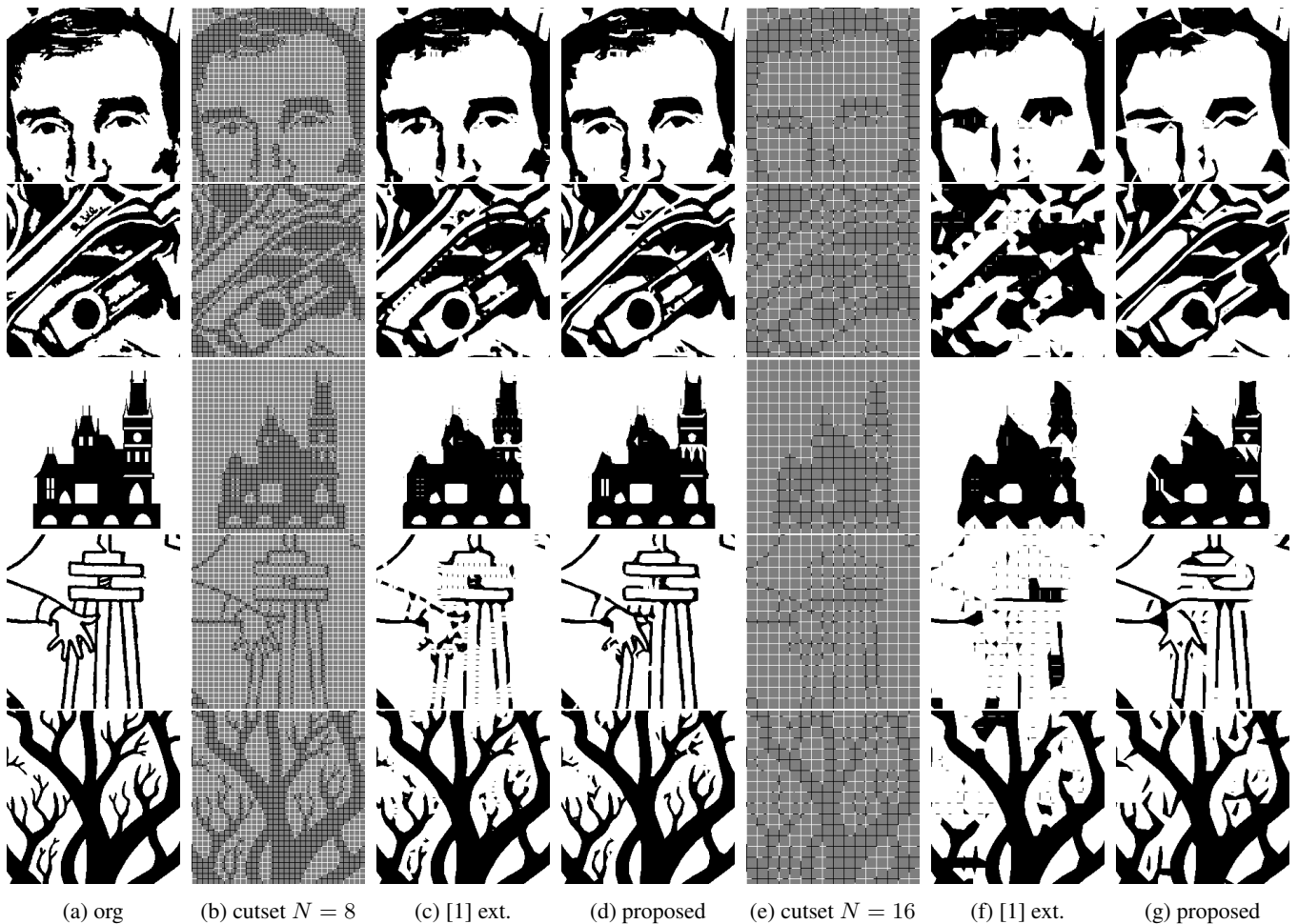[3] Shengxin Zha and Thrasyvoulos N Pappas, "Pattern-based k-level cutset reconstruction," in *International*

| (a) org | (b) cutset $N = 8$ | (c) [1] ext. | (d) proposed | (e) cutset $N = 16$ | (f) [1] ext. | (g) proposed |

Fig. 4: Reconstruction result

Conference on Image Processing (ICIP), Quebec City, Canada, September 2015, IEEE.

[4] Marcelo Bertalmio, Andrea L Bertozzi, and Guillermo Sapiro, "Navier-stokes, fluid dynamics, and image and video inpainting," in *Computer Vision and Pattern Recognition, 2001. CVPR 2001. Proceedings of the 2001 IEEE Computer Society Conference on*. IEEE, 2001, vol. 1, pp. I–355.

[5] Alexandru Telea, "An image inpainting technique based on the fast marching method," *Journal of graphics tools*, vol. 9, no. 1, pp. 23–34, 2004.

[6] Ben Kimia, "A large binary image database," `http://www.lems.brown.edu/~dmc/`, 2002, Accessed: 2015-01-10.